Journal of Engineering and Applied Sciences 5 (6): 394-402, 2010
ISSN: 1816-949X


# Influence of Al Content and Bias Voltage on the Microstructure of $Ti_{1-x}AL_xN$ Hard Coatings

Fisnik Aliaj and Naim Syla
Department of Physics, Faculty of Mathematical and Natural Sciences,
University of Prishtina Mother Theresa, Street 5,
10000 Prishtina, Republic of Kosovo

**Abstract:** Titanium Aluminum Nitride (Ti-Al-N) system is a well established hard coating known for their good physical, chemical and mechanical properties that is used in a variety of fields. The aim of this research is to investigate the influence of bias voltage and aluminum content on the microstructure, chemical composition and the residual stress of Ti-Al-N in order to illuminate the possibility of tailoring the coating properties mentioned above. Four groups of $Ti_{1-x}Al_xN$ coatings were deposited by Cathodic Arc Evaporation (CAE) using powder metallurgical targets of $Ti_{1-xT}Al_{xT}$ with $x_T$ = 0.50, 0.55, 0.60 and 0.66. The coatings were deposited onto cemented carbide (WC-Co) substrates at a temperature of 500°C, at different bias voltages: -25, -50 and -100 V. Structural characterization of the coatings was performed with Glancing Angle X-Ray Diffraction (GAXRD) and Glow Discharge Optical Emission Spectroscopy (GDOES). The microstructure of the coatings changed from predominantly single-phase fcc for *x* between ~0.50 and ~0.60 to dual phase fcc+hcp for x = ~0.66. The residual stress and the stress-free lattice parameter were analyzed using GAXRD and the $\sin^2\Psi$ method was used to evaluate the data. Young's modulus of 500 GPa and Poisson's ratio of 0.3 were utilized in the evaluation. Residual compressive stress increased for about 4 GPa with increasing bias from -25 to -50 V. Further increasing bias from -50 to -100 V resulted only in an increase of about 1GPa. This investigation shows clearly the relations between the target and coating composition where bias is an important parameter.

**Key words:** Bias voltage, cathodic arc evaporation, hard coatings, GAXRD, residual stress, Ti-Al-N

## INTRODUCTION

Ti-Al-N system is a well established hard coating known for their good physical, mechanical and chemical properties that are used in a variety of fields: cutting applications, metal sheet forming, dies and moulds to components in the aerospace and automotive industries (Leyendecker *et al*., 1991; Coll *et al*., 1992; Carlsson and Olsson, 2006) but there is an increasing demand for further development of this coating system. Most of the time, this is done by addition of alloying elements, e.g., Silicon (Si) (Durand-Drouhin *et al*., 2003; Rafaja *et al*., 2007, 2008), Vanadium (V) (Pfeiler *et al*., 2007), Tantalum (Ta) (Pfeiler *et al*., 2008), Yttrium (Y) (Moser and Mayrhofer, 2007) etc., by varying Al content (Inamura *et al*., 1987; Kimura *et al*., 1999; Suzuki *et al*., 2000; Kutschej *et al*., 2005) or by process optimization (Coll *et al*., 1992; Vlasveld *et al*., 2002; Bujak *et al*., 2004; Ahlgren and Blomqvist, 2005). All these different approaches aim on the same thing: improvement of the mechanical properties, oxidation resistance or tribological properties, i.e., in creasing wear resistance and/or lowering the coefficient of friction. Varying the Al content influences primarily, the phase composition which in turn has effects on microstructure and properties of the Ti-Al-N coatings.

For prediction of the phase composition in transition metal aluminum nitrides, Makino (1995) published a theoretical approach where the critical composition for face-centered-cubic (fcc)/hexagonal-close-packed (hcp) was predicted by the two band parameters (hybrid function H and the band gap reduction parameter S), the crystal structure map based on these parameters and the composition factor $f_{inv}$. Based on this approach, it has been calculated (Sugishima *et al*., 1997) that the critical composition for fcc-TiN/hcp-AlN phase transition in the $Ti_{1-x}Al_xN$ system is about x = 0.65. This suggests that the fcc phase would transform to the hcp phase directly when Al content is x = 0.65 in the $Ti_{1-x}Al_xN$ system. But the normal expectation is that we have a two phase region where both phases are present that depends on the technique used to deposit the coatings and is influenced

**Corresponding Author:** Fisnik Aliaj, Department of Physics, Faculty of Mathematical and Natural Sciences, University of Prishtina Mother Theresa, Street 5, 10000 Prishtina, Republic of Kosovo

primarily by the deposition parameters. Experiments performed on the Ti-Al-N coatings deposited using the Arc Ion Plating (AIP) (Kimura *et al*., 1999) consisted of a single fcc phase up to $x \leq 0.6$ and then the phase composition changed abruptly to hcp for $x \geq 0.7$ because of the excess of Al content. The Ti-Al-N coatings deposited using the Ion Beam Assisted Deposition (IBAD) technique (Suzuki *et al*., 2000) consisted of a single fcc phase for Al content up to $x \leq 0.67$. Increasing Al content to x = 0.7 yielded a mixture of fcc and hcp phase whereas for larger Al contents the coating consisted only of hcp phase with wurtzitic type structure. Similar results were obtained by other Physical Vapor Deposition (PVD) techniques (Cramer *et al*., 2001; Rafaja *et al*., 2006). There is one thing in common for all these studies: there is a large region of Al content where the dominating phase is fcc-(Ti, Al)N that may be followed by a narrowly region where both fcc-(Ti, Al)N and hcp-AlN are observed whereas further increasing of Al content the coatings consist mainly of the hcp-AlN phase. Recent calculations of Mayrhofer *et al*. (2006) reports that the critical solubility limit can be varied by 16% from 0.64-0.74 by affecting the Al distribution on the metal sub-lattice. Therefore, the mechanism that influences the Al distribution during film growth will also influence the critical solubility limit.

Another very influential parameter to tailor the microstructure and thus, the properties of Ti-Al-N coatings is the negative substrate bias. The bias voltage during the coating process is a highly influential parameter because it controls the energy of the impinging ions. At low bias voltage levels (0-100 V), the residual compressive stress increases with increasing bias voltage due to a higher defect density which is also connected with an increase in hardness. At higher bias voltages, the ion bombardment induced mobility of atoms which promotes the annihilation of defects, reduces the residual stress and consequently the hardness also drops (Sato *et al*., 2003; Ahlgren and Blomqvist, 2005).

The bias voltage also is a very influential parameter on the chemical composition of the coatings as compared with the cathode used to deposit the coatings. Different research teams (Coll *et al*., 1992; Vlasveld *et al*., 2002) have observed that increasing bias voltage leads to a depletion of the Al content in the coatings. However, a relatively good agreement was between the initial cathode composition and the nucleated Ti-Al-N coating when no bias voltage was applied to the substrate. The depletion of Al content with bias voltage was attributed to a higher degree of ionization in Ti vapor (80%) than Al vapor (50%) emitted from cathodic arc spots. On the other hand, Vlasvled *et al*. (2002) have also observed that with increasing arc current the Al content in the coatings increased. This effect was attributed to the arc spot splitting that is more arc spots which in turn results in an increased evaporation rate of the lower melting point constituent which is Al. In this research, $Ti_{1-x}Al_xN$ hard coatings were deposited by CAE using a hard coating unit from PLATIT. GDOES and GAXRD were used to characterize the structure of the coatings. The emphasis of the research was placed on the effect that Al content x and substrate bias voltage has on the microstructure, composition as well as residual stress in order to illuminate the possibility of tailoring the coating properties. In particular, we illustrate the interplay between chemical composition of the coatings and deposition parameters.

## MATERIALS AND METHODS

**Deposition of the coatings:** Hard coatings of $Ti_{1-x}Al_xN$ with different Al content x were deposited by CAE using a hard coating unit 300 π from PLATIT. The deposition of the coatings was performed in a $N_2$ atmosphere using three cathodes one Central Rotating Cathode (CERC) produced by powder metallurgy and two Lateral Rotating Cathodes (LARC) produced by casting. The dimensions of the rotating cathodes from now on referred to as targets were: Ø 96×510 mm for lateral targets and Ø 110×510 mm for central target as required by deposition apparatus. Variable stoichiometry of the coatings was achieved by using central targets $Ti_{1-xT}Al_{xT}$ with different Al contents: $x_T$ = 0.50, 0.55, 0.60 and 0.66. The bias voltages were -25, -50 and -100 V, respectively. Mirror-polished plates of cemented carbides were utilized as substrates as usual for coatings considered for high temperature applications. The deposition of the coatings consisted of a heating and cleaning procedure after which a thin base layer of TiN was deposited for 5 min using lateral targets made of Ti, at a $N_2$ atmosphere with pressure 0.5-1.0 Pa. The deposition of the main coating was performed for 160 min at a $N_2$ atmosphere with a working pressure of 5 Pa. The current on the target was 300 A and a magnetic field of 2.5 T was used for confinement of the arc discharge. The deposition temperature was approximately 500°C for all runs.

**Microstructure analysis of the coatings:** A detailed microstructure analysis of the coatings comprised the analysis of their chemical and phase composition.

**Chemical composition analysis of the coatings:** The apparatus used in this research to determine the chemical composition of the as deposited coatings was a

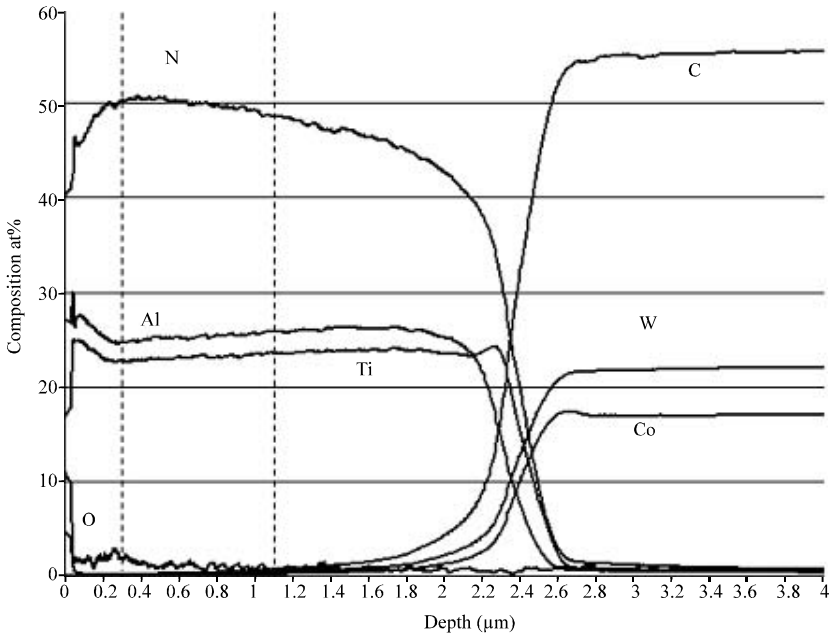


Fig. 1: The GDOES composition profile of the coating deposited using the target $Ti_{0.5}Al_{0.5}$ at a substrate bias of -100 V. The two vertical doted lines denote the range that was taken for the calculation of the averaged at%

commercial surface depth profile GDOES instrument Leco SDP-750 (Leco Technik GmbH, Munich, Germany) that was equipped with a multi-channel polychromator and a Grimm-type GDS. The sputtered area was 4 mm in diameter, the sputtering was performed in constant power mode (U = 900 V and I = 20 mA) and at an Ar flow of 400 sccm. For a more detailed description of the GDOES technique, the reader is referred to Bubert and Jenett (2002). A typical composition profile that was obtained by GDOES for the coating deposited using the target $Ti_{0.5}Al_{0.5}$ at a substrate bias of -100 V (sample 3) is shown in Fig. 1.

**XRD analysis of the coatings:** The phase compositions of the coatings, the stress-free lattice parameter and the residual stress were determined by GAXRD with a constant angle of incidence of $\gamma$ = 3°. The GAXRD experiments were performed on a D8 Advance diffractometer (Bruker AXS) that was equipped by a sealed X-ray tube with copper anode ($\lambda$ = 0.15418 nm) by a parabolic Gobel mirror in the primary beam and by a Soller collimator with the acceptance angle of 0.12° and a flat LiF monochromator (which changed the K$\alpha$2/K$\alpha$1 intensity ratio to 0.08) that were situated in the diffracted beam in front of the scintillation detector. Residual stress and stress-free lattice parameter were analyzed using GAXRD and the evaluation of the data was based on the so-called $\sin^2\psi$ method (Rickerby *et al*., 1989; Perry and Jagner, 1989; Noyan *et al*., 1995). In this analysis, it is assumed that the stress state which exists within the coating is of the biaxial stress and the measured value of the strain is related to the residual stress according to Eq. 1:

$$\varepsilon_{hkl} = \frac{d_{hkl} - d_0}{d_0} = \frac{1+\nu}{E}\sin^2\Psi - 2\sigma\frac{\nu}{E} \quad (1)$$

Where:

$d_{hkl}$ = The interplanar spacing for the hkl reflection
$d_0$ = The stress-free interplanar spacing
$\sigma$ = The residual stress
E = The Young's modulus
$\nu$ = The Poisson's ratio
$\Psi$ = The angle between diffracting plane normal and the sample surface normal and is related to the incidence angle $\gamma$ and the diffracting angle $\theta$ according to equation $\Psi = \theta - \gamma$

The individual interplanar spacing $d_{hkl}$ which corresponded to cubic phase were determined by fitting individual peaks with Pearson 7 function using a peak-by-peak method (Birkholz, 2006; Guine-bretiere, 2007). Then, the individual lattice parameters of the cubic phase $a_{hkl}$ were calculated according to Eq. 2:

$$a_{hkl} = \sqrt{h^2 + k^2 + l^2}\, d_{hkl} \quad (2)$$

After determining the individual lattice parameters then, the stress-free lattice parameters in the cubic phase were calculated according to Eq. 3 (Rafaja *et al*., 2006):

$$a_0 = (a_{\parallel} - a_{\perp})\frac{2\nu}{1+\nu} + a_{\perp} \quad (3)$$

Where, $a_{\perp}$ and $a_{\parallel}$ are the cubic lattice parameters perpendicular and parallel to the sample surface which are directly obtained from the $\sin^2\psi$-plot at $\sin^2\psi = 0$ and $\sin^2\psi = 1$, respectively. Residual stress of the coatings was calculated from the slope of the least square fit of the individual lattice parameters $a_{hkl}$ on the function $\sin^2\psi$ according to Eq. 4:

$$\sigma = \frac{\text{slope} \cdot E}{a_0(1+\nu)} \quad (4)$$

Young's modulus of 500 GPa and Poisson's ratio of 0.3 were utilized in the evaluation of residual stress and stress-free lattice parameter.

## RESULTS AND DISCUSSION

**Chemical composition of the coatings:** Although, the atomic compositions deduced from GDOES data analysis cannot be considered as absolute values, the compositional results obtained for different samples show that the ratio of nitrogen to metal atoms [N]/([Al]+[Ti]) is between 0.95 and 1.39 and that the [Al]/([Al]+[Ti]) atomic ratio in the coatings was measured to be higher than that in the evaporation target (Table 1).

Figure 2 shows the variation of the [Al]/([Al]+[Ti]) atomic ratio in the coating (x) as a function of the [Al]/([Al]+[Ti]) atomic ratio in the target ($x_T$). Similar results were obtained for Ti-Al-N coatings deposited by other PVD techniques (Inamura *et al*., 1987; Rauch *et al*., 2000; Suzuki *et al*., 2000; Kutschej *et al*., 2005). The increase of the Al atomic percent was attributed to the lower melting point for Al than Ti (Suzuki *et al*., 2000). Since, the chemical composition of the coatings is different from that of the targets that were used to deposit the coatings, we use the following naming convention to refer to particular group of coatings: coatings deposited from the target $Ti_{0.50}Al_{0.50}$, we refer to as group 1 coatings, coatings deposited from the target $Ti_{0.45}Al_{0.55}$ as group 2 coatings, coatings deposited from the target $Ti_{0.40}Al_{0.60}$ as group 3 coatings and finally coatings deposited from the target $Ti_{0.34}Al_{0.66}$ as group 4 coatings.

Besides that the Al content in the coatings is different from that of the targets, we have also observed that the [Al]/([Al]+[Ti]) atomic ratio of the coatings (x) increases with increasing bias voltage ($V_s$) and that this increase is linear for all four groups of coatings (Fig. 3). From Fig. 3, we see that the values of the intercept are very close to Al content of the targets ($x_T$).

The intercept has the meaning of the Al content in the coating that would have been obtained if the coatings were to be deposited without any bias voltage. This result is in good agreement with the work of others (Freller and Haeseller, 1987; Coll *et al*., 1991) for Ti-Al-N coatings deposited by cathodic arc evaporation. Both research teams have observed a relatively good agreement between the initial cathodic composition and the nucleated Ti-Al-N films when no bias voltage was applied to the substrate. Fitting the data points with straight lines reveals that the slope increases with increasing Al content of the target. Therefore, the results shown in Fig. 3 can be summed up with the following Eq. 5:

$$x = a_T|V_s| + x_T \quad (5)$$

Where:

$x_T$ = Al content of the target
$x$ = Al content of the coating
$V_s$ = The negative substrate bias
$a_T$ = The slope that depends on the Al content of the target and its physical meaning is that of a rate of increase of the Al content in the coating per unit bias voltage

For every target ($x_T$, $a_T$) and for every value of the substrate bias ($V_s$), the coating composition (x) is governed by the Eq. 5 in the range of bias voltages investigated in this research. This difference between Al content in the coating and Al content in the target and

Table 1: GDOES data analysis

| Sample number | Bias voltage | [Al]/([Al]+[Ti]) target ($x_T$) | [Al]/([Al]+[Ti]) coating (x) | [N]/([Al]+[Ti]) coating | Coating thickness | [O] at (%) |
|---|---|---|---|---|---|---|
| 1 | -25 V | 0.50 | 0.514 (6) | 0.955 (19) | 2.4 (1) | 1.7 (5) |
| 2 | -50 V | 0.50 | 0.517 (8) | 1.040 (27) | 2.5 (2) | 1.2 (5) |
| 3 | -100 V | 0.50 | 0.522 (5) | 1.032 (23) | 2.5 (1) | 1.1 (3) |
| 4 | -50 V | 0.55 | 0.561 (17) | 1.102 (58) | 2.5 (1) | 3.5 (9) |
| 5 | -100 V | 0.55 | 0.570 (12) | 1.005 (52) | 2.3 (2) | 2.0 (8) |
| 6 | -50 V | 0.60 | 0.608 (9) | 1.131 (35) | 2.5 (1) | 1.2 (3) |
| 7 | -100 V | 0.60 | 0.618 (3) | 1.089 (16) | 2.4 (2) | 0.8 (3) |
| 8 | -25 V | 0.66 | 0.659 (5) | 1.219 (28) | 2.7 (3) | 0.3 (2) |
| 9 | -50 V | 0.66 | 0.665 (12) | 1.386 (53) | 2.7 (3) | 0.7 (4) |
| 10 | -100 V | 0.66 | 0.676 (3) | 1.234 (3) | 2.5 (2) | 0.7 (6) |

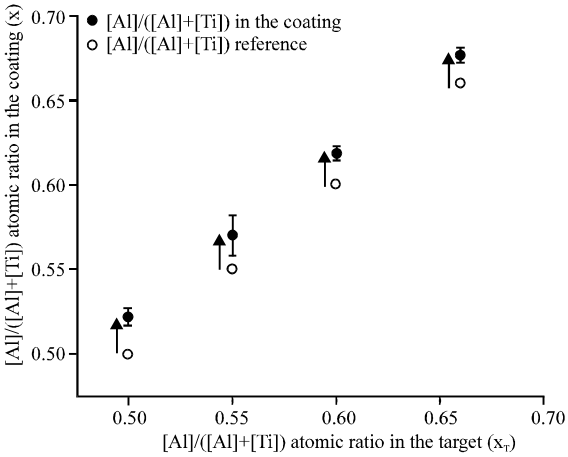


Fig. 2: [Al]/([Al]+[Ti]) atomic ratio of the coatings as a function of the [Al]/([Al]+[Ti]) atomic ratio of the targets, for the coatings deposited at -100 V bias. Similar result is obtained for the coatings deposited at -25 and -50 V bias

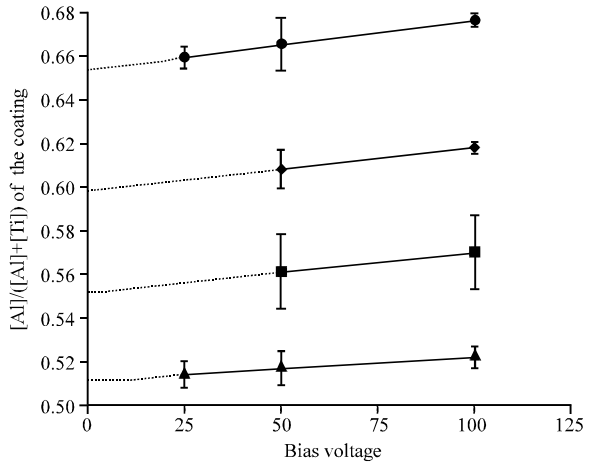


Fig. 3: [Al]/([Al]+[Ti]) atomic ratio of the coatings (x) as a function of the bias voltage. Filled triangles represent group 1 coatings, filled rectangles group 2 coatings, filled diamonds group 3 coatings and filled circles group 4 coatings. Solid lines are least squares fit to the data points. Dashed lines are extrapolations at 0 bias. Error bars are standard deviations obtained from GDOES analysis

the dependence on bias voltage and on the target composition, at first glance appears to be a disadvantage of the cathodic arc evaporation. However, all this information can be actually used to optimize the arc deposition of the coatings. In practice in arc evaporation process, a fixed bias voltage is used. Then, the observed enrichment of Al in the coatings can be overcome by using an adapted depletion of Al in the target. Moreover, the dependence of the Al content in the coating on the bias voltage offers the great advantage of varying the composition of Ti-Al-N coating during film growth by simply changing the bias voltage and using the same cathode throughout. All these results point out the importance of the CAE as a very versatile technique for depositing Ti-Al-N hard coatings.

## Crystallographic structure

**Phase composition of the coatings:** Figure 4 shows the crystallographic structure of the as deposited $Ti_{1-x}Al_xN$ coatings investigated in this research as obtained from GAXRD. Vertical doted lines indicate the expected peak positions for the respective phases. For the phases fcc-TiN, fcc-AlN, hcp-AlN and hcp-WC, the values for the peak positions were taken from powder diffraction file (PDF-2). For the phase fcc-(Ti, Al)N, the peak position were calculated from Bragg's law using a value of a = $4.19.10^{-10}$ m for the lattice parameter taken from (Inamura *et al*., 1987).

All the fcc-(Ti, Al)N peaks of the coatings are shifted to higher/lower diffraction angles than the standard value of fcc-TiN/fcc-AlN. This is due to the incorporation of the smaller Al atoms into the fcc-TiN lattice. Thus, the results from GAXRD confirm limited solubility of Al in the host structure of the TiN. For group 1, 2 and 3 coatings, the dominating phase is fcc-(Ti, Al)N while group 4 coatings exhibit a mixture of fcc-(Ti, Al)N and hcp-AlN with wurtzitic type structure.

The variation of the phases from the fcc structure to the two phase mixture (fcc+hcp) in Ti-Al-N system is consistent with the results obtained from the films deposited using r.f.-plasma assisted magnetron sputtering (Zhou *et al*., 1999), DC magnetron sputtering system (Kutschej *et al*., 2005), Arc Ion Plating (AIP) and cathodic arc evaporation (Rafaja *et al*., 2006).

In coatings were the dominating phase is fcc-(Ti, Al)N (group 1, 2 and 3 coatings) traces of fcc-AlN and hcp-AlN were detected by XRD. In Fig. 5, the fcc-TiN peak is as a result of the deposited thin base layer. The lattice parameter of the fcc-AlN phase (calculated by means of Bragg's law using as a wavelength $\lambda$ = 0.15418 nm) was found to be between 0.4070 and 0.4123 nm which is in relatively good agreement with PDF-2.

The hcp-AlN peak with indices 202 located at approximately 82 degrees $2\theta$ is in good agreement with PDF-2. We have observed that with increasing bias voltage this peak gets broader probably because of the reduction of the crystallite size.

**Stress-free lattice parameter:** The stress-free lattice parameters in the cubic phase, $a_0$ calculated from the $\sin^2\psi$-plots are compared with the anticipated Vegard-like dependence of the intrinsic lattice parameter on the

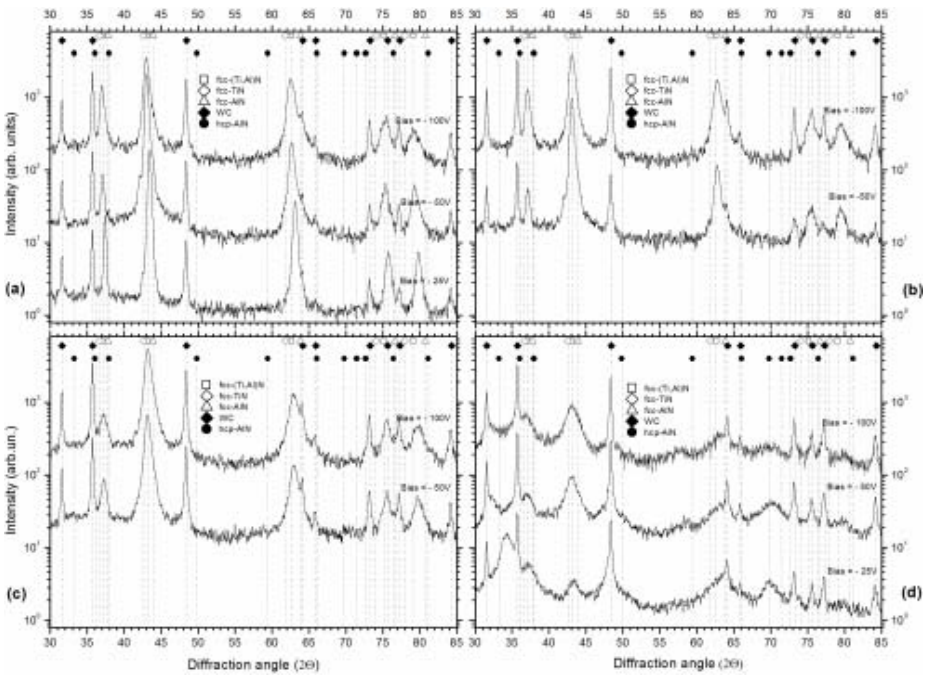


Fig. 4: Crystallographic structure of the coatings as obtained from GAXRD. a-d) group 1-4 coatings, respectively

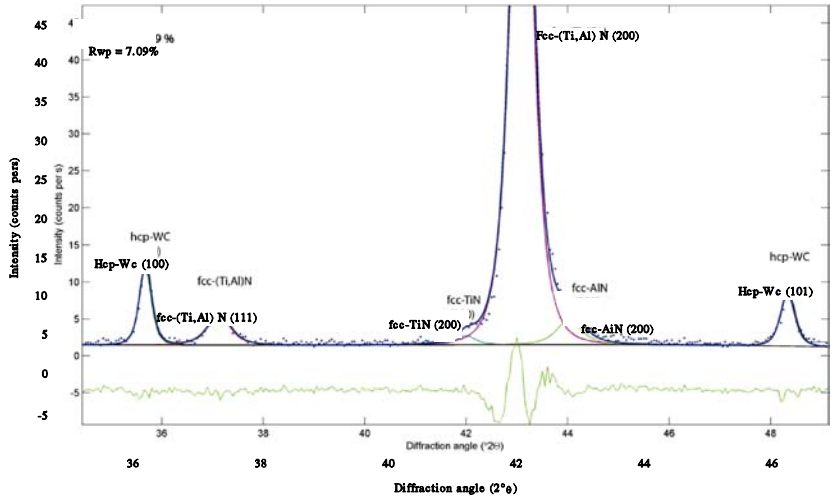


Fig. 5: The process diffraction pattren of a coating deposited from target $Ti_{0.45}Al_{0.55}$ at bias voltage -50 V, showing peaks from subtrate and coating. fcc-TiN is a result of a deposited thin base layer. fcc-peak located at approximately 44 degrees implies that cubic AIN also formed in the coatings. Similar peak were found in almost all of the coatings where fcc-(Ti, Al)N was the dominating phase

overall Ti contents in fcc-(Ti, Al)N which is shown in Fig. 6. The stress-free lattice parameter in fcc-(Ti, Al)N decreases with increasing Al contents in the coatings as anticipated. A deviation was observed for sample 1, a coating deposited at -25 V bias from a target $Ti_{0.50}Al_{0.50}$. This is because of much lower nitrogen content for this coating (Table 1).

The measured lattice parameters are higher as compared with the lattice parameters anticipated from the measured overall chemical composition. Therefore, some Al from the total Al contents measured from GDOES must be missing in fcc-(Ti, Al)N for all group of coatings. Consequently, fcc-(Ti, Al)N has higher Ti and lower Al content than it corresponds to the overall chemical

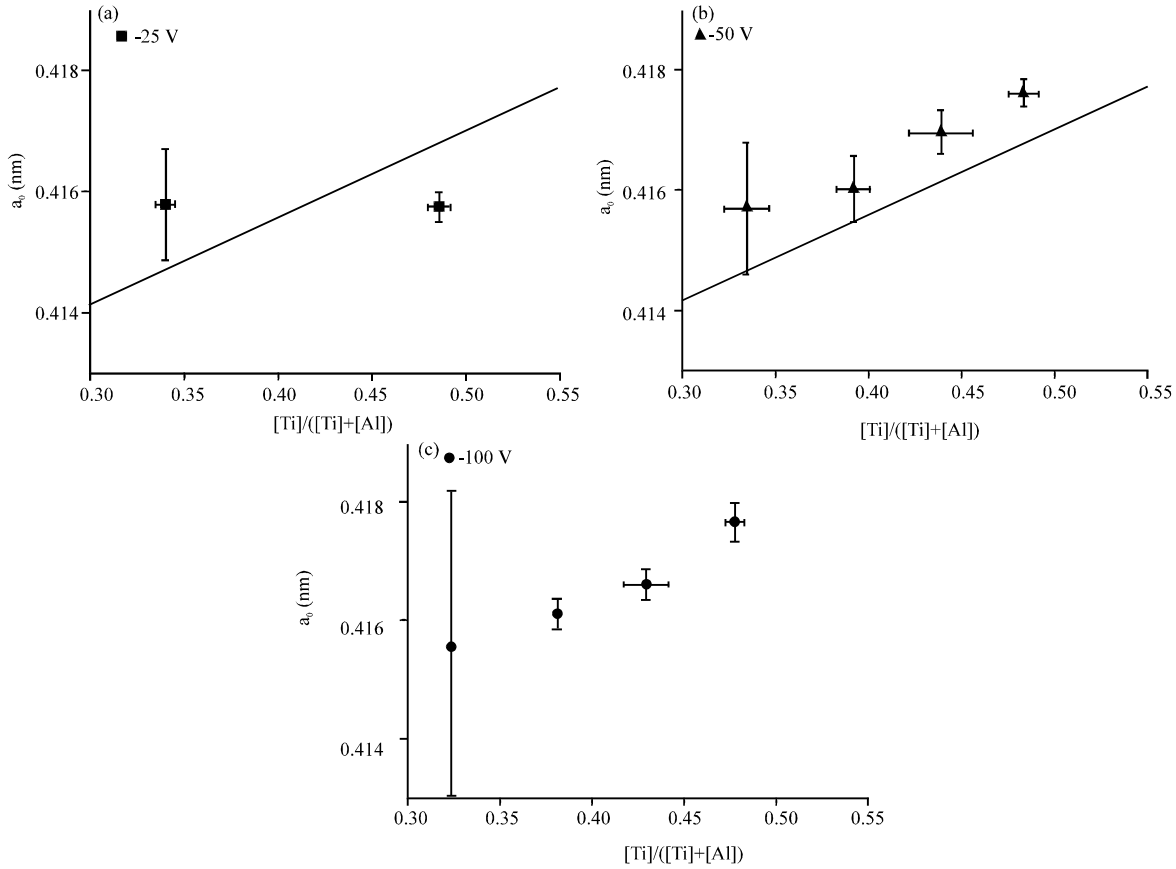


Fig. 6: The dependence of the stress-free lattice parameter of the fcc-(Ti, Al)N, $a_0$ on the stoichiometry ratio [Ti]/([Ti]+[Al]). Filled symbols represent coatings where fcc-(Ti, Al)N is the dominating phase, half-filled symbols represent coatings where fcc-(Ti, Al)N and hcp-AlN are present. The vertical dotted lines represent the Ti content in the target; the solid line represents the anticipated Vegard like dependence and the equation for this line was taken from (Rafaja *et al*., 2008)

composition of the individual samples obtained from the GDOES. The lower Al contents in fcc-(Ti, Al)N in comparison with the overall chemical composition results in a higher lattice parameter of this phase in comparison with the lattice parameter anticipated for the overall chemical composition. For group 4 coatings where both phases are present that is fcc-(Ti, Al)N and hcp-AlN, the departure of the stress-free lattice parameter from the anticipated Vegard-like dependence can be understood as a measure of the decomposition of $Ti_{1-x}Al_xN$ into fcc-(Ti, Al)N and hcp-AlN (Rafaja *et al*., 2006).

The departure of lattice parameters from the anticipated Vegard-like dependence for group 1-3 coatings is in agreement with the results obtained from the GDOES analysis. According to GDOES results, Al content in the coatings is higher than Al content in the target. Besides this, Al increases with increasing bias voltage. Therefore, it is highly reasonable that the hcp-AlN and possibly fcc-AlN has also formed in these groups of coatings during deposition in small amounts and small crystallite sizes which was in most of the cases also detected by XRD, giving as a result a slightly higher stress-free lattice parameters than the anticipated Vegard-like dependence. Therefore in this group of coatings, the additional Al does not incorporate into Ti-Al-N; instead it contributes to the formation of AlN phase. This statement is in agreement with the concept of free energy where the formation of AlN phase requires lower energy than further incorporation of Al atoms in the Ti-Al-N structure (Hugosson *et al*., 2003).

**Residual stress:** The residual stress in all the coatings was compressive. As it is shown in Fig. 7, there is an increase in compressive residual stress with increasing bias voltage for all groups of coatings. The largest values of residual stress were obtained for coatings deposited using a target with composition $Ti_{0.34}Al_{0.66}$. An especially large increase of about 4 Gpa is observed

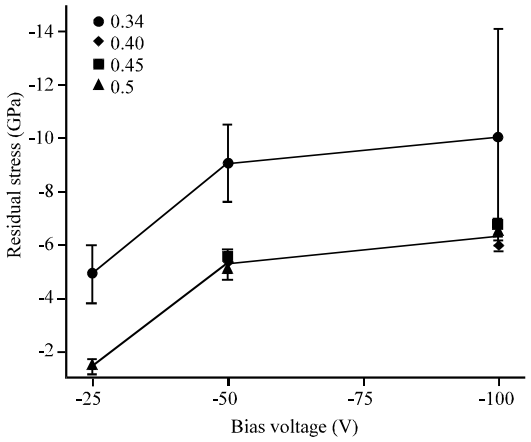


Fig. 7: The dependence of the residual stress on the negative substrate bias. The numbers in the legend represent the Ti content in the targets used to deposit the coatings. The lines are guide for the eye

between -25 and -50 V bias for all groups of coatings while increasing bias voltage from -50 to -100 V resulted only in an increase of about 1GPa. Figure 7 shows that the dependence of residual stress on bias voltage is the same for all groups of coatings. Since, there was no coatings deposited at -25 V bias using targets $Ti_{0.45}Al_{0.55}$ and $Ti_{0.40}Al_{0.60}$, the dependence of residual stress on bias voltage in the range between -25 and -50 V can only be anticipated based on the dependence observed for coatings deposited using targets $Ti_{0.50}Al_{0.50}$ and $Ti_{0.34}Al_{0.66}$.

An increase of residual stress with increasing bias voltage is a well reported phenomenon and is due to the increase of energy of the bombarding ions with increase of substrate bias voltage. This ion bombardment has been linked to a shot peening process which generates higher defect concentration with increasing shot intensity and can lead to a change in microstructure from one that is open and columnar Zone-1 type microstructure to a dense Zone-T type microstructure (Vlasvled *et al*., 2001). (Windischmann, 1992) postulated that higher levels of ion bombardment should lead to saturation in defect concentration, i.e., compressive stress saturation, before yielding due to plastic flow. This may indeed be the case in this study. The relatively low increase of residual stress between -50 and -100 V could be that the coatings are at this saturation region.

## CONCLUSION

$Ti_{1-x}Al_xN$ coatings with variable stoichiometry x were deposited by Cathodic Arc Evaporation (CAE). Al content in the coatings was different from Al content in the targets that were used to deposit the coatings. Al content in the coatings increased with increasing bias voltage. The relationship is linear: $x = a_T|V_s|+x_T$. The microstructure of the coatings changed from predominantly single-phase fcc for x between ~0.50 and ~0.60 to dual phase fcc+hcp for x = ~0.66. The residual strees was found to be compressive in all the coatings and increased for about 4 Gpa with increasing bias from -25 to -50 V. Further increasing bias from -50 to -100 V resulted only in an increase of about 1 GPa.

## ACKNOWLEDGEMENTS

The researchers thank the DAAD (German Academic Exchange Service) for the financial support obtained for the educational journey to Freiberg, Germany.

## REFERENCES

Ahlgren, M. and H. Blomqvist, 2005. Influence of bias variation on residual stress and texture in TiAlN PVD coatings. Surface Coatings Technol., 200: 157-160.

Birkholz, M., 2006. Thins Film Analysis by X-Ray Scattering. Wiley-VCH Verlag, GmBH, Weinheim.

Bubert, H. and H. Jenett, 2002. Surface and Thin Films Analysis: Principles, Instrumentation, Applications. Wiley-VCH Verlag GmBH, Weinheim.

Bujak, J., J. Walkowicz and J. Kusinski, 2004. Influence of the nitrogen pressure on the structure and properties of (Ti,Al)N coatings deposited by cathodic vacuum Arc PVD process. Surface Coatings Technol., 180-181: 150-157.

Carlsson, P. and M. Olsson, 2006. PVD coatings for sheet metal forming processes: A tribological evaluation. Surface Coatings Technol., 200: 4654-4663.

Coll, B.F., P. Sathrum, R. Fontana, J.P. Peyre and D.D.M. Benmalek, 1992. Optimization of arc evaporated (Ti,Al)N film composition for cutting tool applications. Surface Coatings Technol., 52: 57-64.

Coll, B.F., R. Fontana, A. Gates and P. Sathrum, 1991. (Ti---Al)N advanced films prepared by arc process. Mater. Sci. Eng., A140: 816-824.

Cramer, R., K. Reicherta and D. Neuschütz, 2001. A composition spread approach to the optimization of (Ti,Al)N hard coatings deposited by DC and bipolar pulsed magnetron sputtering. Surface Coatings Technol., 142-144: 642-648.

Durand-Drouhin, A., A.E. Santanaa, A. Karimi, V.H. Derflingerb and A. Schutze, 2003. Mechanical properties and failure modes of TiAl(Si)N single and multilayer thin films. Surface Coatings Technol., 163-164: 260-266.

Freller, H. and H. Haeseller, 1987. $Ti_xAl1-_xN$ films deposited by ion plating with an arc evaporator. Thin Solid Films, 153: 67-74.

Guine-bretiere, R., 2007. X-Ray Diffraction by Polycrystalline Materials. ISTE Ltd., London.

Hugosson, H.W., H. Hogberg, M. Algren, M. Rodmar and T.I. Selinder, 2003. Theory of the effects of substitutions on the phase stabilities of $Ti_{1-x}Al_xN$. J. Applied Phys., 93: 4505-4511.

Inamura, S., K. Nobugai and F. Kanamaru, 1987. The preparation of NaCl-type Ti1-xAlxN solid solution. J. Solid State Chem., 68: 124-127.

Kimura, A., H. Hasegawaa, K. Yamadaa and T. Suzuki, 1999. Effects of Al content on hardness, lattice parameter and microstructure of $Ti_{1-x}Al_xN$ films. Surface Coatings Technol., 120-121: 438-441.

Kutschej, K., P.H. Mayrhoferb, M. Kathreinc, P. Polcikd, R. Tessadrie and C. Mitterer, 2005. Structure, mechanical and tribological properties of sputtered Ti1-xAlxN coatings with 0.5=x=0.75. Surface Coatings Technol., 200: 2358-2365.

Leyendecker, T., O. Lemmera, S. Essera and J. Ebberink, 1991. The development of the PVD coating TiAlN as a commercial coating for cutting tools. Surface Coatings Technol., 48: 175-178.

Makino, Y., 1995. Structural mapping of intermetallic compounds and bond character. Mater. Sci. Eng. A, 192-193: 77-82.

Mayrhofer, P.H., D. Music and J.M. Schneider, 2006. Influence of the AI distribution on the structure, elastic properties and phase stability of supersaturated Ti~1~~~xAl~xN. J. Applied Phys., Vol. 100. http://direct.bl.uk/bld/PlaceOrder.do?UIN=199599690&ETOC=RN&from=searchengine.

Moser, M. and P.H. Mayrhofer, 2007. Yttrium-induced structural changes in sputtered $Ti_{x-x}Al_xN$ thin films. Scripta Materialia, 57: 357-360.

Noyan, I.C., T.C. Huang and B.R. York, 1995. Residual stress/strain analysis in thin films by X-ray diffraction. Crit. Rev. Solid State Mater. Sci., 20: 125-177.

Perry, A.J. and M. Jagner, 1989. Residual stress in physically vapor deposited films: A study of deviations from elastic behavior. Thin Solid Films, 171: 197-216.

Pfeiler, M., G. A. Fontalvo, J. Wagner, K. Kutschej and M. Penoy *et al*., 2008. Arc evaporation of Ti–Al–Ta–N coatings: The effect of bias voltage and ta on high-temperature tribological properties. Tribol. Lett., 30: 91-97.

Pfeiler, M., K. Kutschejb, M. Penoyc, C. Michottec, C. Mittererb and M. Kathrein, 2007. The influence of bias voltage on structure and mechanical/tribological properties of arc evaporated Ti-Al-V-N coatings. Surface Coatings Technol., 202: 1050-1054.

Rafaja, D., A. Poklada, V. Klemma, G. Schreibera, D. Hegera and M. Síma, 2007. Microstructure and hardness of nanocrystalline $Ti_{1-x-y}Al_xSi_yN$ thin films. Mater. Sci. Eng., 462: 279-282.

Rafaja, D., A. Poklada, V. Klemma, G. Schreibera, D. Hegera, M. Símab and M. Dopita, 2006. Some consequences of the partial crystallographic coherence between nanocrystalline domains in Ti-Al-N and Ti-Al-Si-N coatings. Thin Solid Films, 514: 240-249.

Rafaja, D., C. Wustefelda, M. Dopitaa, V. Klemma, D. Hegera, G. Schreibera and M. Sima, 2008. Formation of defect structures in hard nanocomposites. Surface Coatings Technol., 203: 572-578.

Rauch, Y.J., C. Rousselotb, N. Martinb, C. Jacquota and J. Takadoum, 2000. Characterization of $(Ti_{1-x}Al_x)N$ films prepared by radio frequency reactive magnetron sputtering. J. Eur. Ceramic Soc., 20: 795-799.

Rickerby, D.S., A.M. Jones and B.A. Bellamy, 1989. X-ray diffraction studies of physically vapour-deposited coatings. Surface Coatings Technol., 37: 111-137.

Sato, K., N. Ichimiyab, A. Kondoa and Y. Tanaka, 2003. Microstructure and mechanical properties of cathodic arc ion-plated (Al,Ti)N coatings. Surface Coatings Technol., 163-164: 135-143.

Sugishima, A., H. Kajiokaa and Y. Makino, 1997. Phase transition of pseudobinary Cr-Al-N films deposited by magnetron sputtering method. Surface Coatings Technol., 97: 590-594.

Suzuki, T., Y. Makino, M. Samandi and S. Miyake, 2000. Microstructure and secular instability of the (Ti1-x,Alx)N films prepared by ion-beam-assisted-deposition. J. Mater. Sci., 35: 4193-4199.

Vlasveld, A.C., S.G. Harrisa, E.D. Doylea, D.B. Lewisb and W.D. Munz, 2002. Characterisation and performance of partially filtered arc TiAlN coatings. Surface Coatings Technol., 149: 217-224.

Windischmann, H., 1992. Intrinsic stress in sputter-deposited thin films. Crit. Rev. Solid State Mater. Sci., 17: 547-596.

Zhou, M., Y. Makinoa, M. Noseb and K. Nogi, 1999. Phase transition and properties of Ti-Al-N thin films prepared by r.f.-plasma assisted magnetron sputtering. Thin Solid Films, 339: 203-208.